International Journal of Heat and Mass Transfer 52 (2009) 4229–4235

Contents lists available at ScienceDirect

International Journal of Heat and Mass Transfer

journal homepage: www.elsevier.com/locate/ijhmt

Radiative heat transfer in a participating medium with specular–diffuse surfaces

Hong-Liang Yi [a], Bing Zhen [a,b], He-Ping Tan [a,*], Timothy W. Tong [c]

[a] School of Energy Science and Engineering, Harbin Institute of Technology, Harbin 150001, PR China
[b] School of Construction and Refrigeration Engineering, Harbin University of Commerce, Harbin 150028, PR China
[c] The HongKong Polytechnic University, HongKong, PR China

ARTICLE INFO

Article history:
Received 6 February 2008
Received in revised form 10 March 2009
Accepted 9 April 2009
Available online 27 May 2009

Keywords:
Radiative transfer coefficients
Hybrid ray-tracing method
Anisotropic scattering

ABSTRACT

The results obtained by ray-tracing method can be regarded as benchmarks for its good accuracy. However, up to now, this method can be only used to solve radiative transfer within medium confined between two specular surfaces or two diffuse surfaces. This article proposes a hybrid ray-tracing method to solve the radiative transfer inside a plane-parallel absorbing–emitting–scattering medium with one specular surface and another diffuse surface (S–D surfaces). By the hybrid ray-tracing method, radiative transfer coefficients (RTCs) for S–D surfaces are deduced. Both surfaces of the medium under consideration are considered to be semitransparent or opaque. This paper examines the effects of scattering albedo, opaque surface emissivity and anisotropically scattering on steady-state heat flux and transient temperature fields. From the results it is found that the effects of anisotropic scattering is more for a bigger optical thickness medium; and keeping other optical parameters unchanged, anisotropic scattering affects transient temperature distributions so much in a small refractive index medium.

1. Introduction

Radiative heat transfer or coupled heat transfer by radiation and conduction plays an important role in many industrial applications. These applications includes radiative cooling of space droplet radiator, infrared heating and infrared drying, optical crystals growth, ceramic components for high temperature use, glass forming for manufacturing and tempering of glass windows, highly backscattering protective insulation systems for reentry into atmosphere, porous burners and insulation systems, measurement for the thermal characterization of semitransparent materials as well as selected high temperature components in advanced aircraft engines. The key to coupled radiation and conduction is seeking solution to radiative transfer problem. The precise prediction of radiative heat transfer is indispensable to improve their design, so an accurate solution method for radiative transfer equation (RTE) has been demanded.

There are many different methods of obtaining solutions of the RTE as reported in the literature. For instance, there are zone method [1], Monte Carlo method (MCM) [2], P–N spherical harmonics method [3], discrete ordinates method (DOM) [4], discrete transfer method (DTM) [5], finite-volume method (FVM) [6], finite element method (DOM) [7], meshless method [8], etc.

Much of the previous work on radiative heat transfer only considered purely absorbing or isotropic scattering. However, it is well known that in the medium including real particles, fibers, or impurities, the anisotropic scattering of thermal radiation can play a significant role on overall heat transfer. Consequently it is necessary to consider anisotropic scattering effects in radiative heat transfer. Much attention has been focused by many researchers on this problem [9–15].

As we know, typical numerical methods for radiative transfer are the finite-volume method (FVM), the discrete ordinates method (DOM), the discrete transfer method (DTM), the finite element method (FEM) and the Monte Carlo method (MCM). Generally, most of them will produce errors, the ray effect and false scattering. Ref. [16] pointed out that the false scattering was generated by the discretization of the derivative term of radiative intensity along the space coordinate, and the ray effect was produced by the discretization of the solid angle. So the false scattering exists in the FVM, FEM and DOM, and the ray effect exists in the FVM, FEM, DOM, and DTM [16]. The advantage of the ray-tracing method is that when solving radiative transfer equation, the radiative intensity does not need to be discretized along the space coordinate, and the solid angle need not be discretized either but is directly integrated. Thus, the method completely avoids the ray effect and the false scattering, and the results obtained by this method can be regarded as benchmarks for its good accuracy. Furthermore, the physical meaning of this method is clear, simple and visual, and it can well reveal the physical essence of the radiative transfer.

Using the ray-tracing method, previous work can but solve the radiative transfer in the medium having two specular surfaces [17–20] or two diffuse surfaces [21]. For the medium having one

* Corresponding author. Tel.: +86 451 86412028; fax: +86 451 86413208.
E-mail addresses: tanheping77@yahoo.com.cn, tanheping@hit.edu.cn (H.-P. Tan).

0017-9310/$ - see front matter © 2009 Elsevier Ltd. All rights reserved.
doi:10.1016/j.ijheatmasstransfer.2009.04.009

Nomenclature

C	heat capacity per unit volume of the medium, J m^{-3} K^{-1}
h_1, h_2	convective heat transfer coefficient at surfaces of S_1 and S_2, respectively, W m^{-2} K^{-1}
H_1, H_2	convection–radiation parameter, $H_1 = h_1/\sigma T^3$ and $H_2 = h_2/\sigma T_r^3$
L	thickness of the medium, m
k	thermal conductivity of the medium, W m^{-1} K^{-1}, n = 1, 2
k_{ie}, k_{iw}	harmonic mean thermal conductivity at interface ie and iw of control-volume i, respectively
N	$k/(4\sigma T_i^3 L)$, conduction–radiation parameter of the medium
M_t	total number of control-volumes of the medium
n	refractive index of the medium
$q^r_{i,e}$, $q^r_{i,w}$	radiative flux passing through the right and the left interface of control-volume i, respectively
q^t	total heat flux of radiation and conduction at steady-state
S_1, S_2	boundary surfaces
$S_{-\infty}$, $S_{+\infty}$	black surfaces representing the surroundings
(S_uS_v), (S_uV_j), (V_jS_u), (V_iV_j)	absorbing RTCs of surface vs. surface, surface vs. volume, volume vs. surface and volume vs. volume
$[S_uS_v]$, $[S_uV_j]$, $[V_jS_u]$, $[V_iV_j]$	scattering RTCs of surface vs. surface, surface vs. volume, volume vs. surface and volume vs. volume
T	absolute temperature, K
T_{g1}, T_{g2}	gas temperatures for convection, K
T_r, T_0	reference temperature, initial temperature, K
$T_{-\infty}$, $T_{+\infty}$	temperatures of black surroundings $S_{-\infty}$ and $S_{+\infty}$, respectively, K
t, Δt, t^*	physical time, s; time interval, s; dimensionless time, $(4\sigma T_r^3/CL)t$
x	coordination or distance along the direction of medium thickness, m
β	common ratio of a geometric progression
Δx	thickness of each control-volume of the medium, m
$(\delta x)_{ie}$, $(\delta x)_{iw}$	distance between nodes i and $i+1$ and between i and $i-1$, respectively
ε_1, ε_2	emissivities of surfaces S_1 and S_2, respectively
η	$1-\omega$
κ	extinction coefficient of the medium, m^{-1}
ρ_1, ρ_2	reflectivities of the opaque surfaces S_1 and S_2, respectively
$\rho_{2,in}$, $\rho_{2,out}$	diffuse reflectivities of the semitransparent surface S_2 facing the medium and surrounding, respectively
σ	Stefan–Boltzmann constant = 5.6696×10^{-8} W m^{-2} K^{-4}
τ	optical thickness, equal to κL
Φ^r_i	radiative heat source of the control-volume i
ω	scattering albedo of the medium

Subscripts

ie, iw	right and left interface of control-volume i
$-\infty$, $+\infty$	$S_{-\infty}$ and $S_{+\infty}$ denoting black surroundings

Superscript

r	radiation

specular surface and another diffuse surface (S–D surfaces), the radiative transfer problem has not been solved by this method. In this paper, according to the directional reflection behavior of the specular surface and hemispherical reflection behavior of the diffuse surface, we develop a hybrid tracing scheme based on the ray-tracing method to solve the radiative transfer in a participating medium having S–D surfaces. By this method the RTCs for the medium with such reflecting characteristics are also deduced. Local radiative heat source in the energy equation, expressed in terms of RTCs, is deduced using the nodal analyzing method. The effects of scattering albedo, opaque surface emissivity and anisotropically scattering on steady heat flux and transient temperature fields are investigated.

2. Basic equations and boundary conditions

We consider a plane-parallel participating medium with its thickness of L. Both boundary surfaces of the medium are supposed to be semitransparent or opaque. The left surface S_1 is specular and the right one S_2 is diffuse. The medium is irradiated by two black surfaces $S_{-\infty}$ and $S_{+\infty}$, indicating the surrounding of temperatures $T_{-\infty}$ and $T_{+\infty}$, respectively. Between S_1 and $S_{-\infty}$ and between S_2 and $S_{+\infty}$ are convective gases with temperatures of T_{g1} and T_{g2}. Along the medium thickness, it is divided into M_t control-volumes, and the total number of nodes is $M_t + 2$, with node 0 locating S_1 and node $M_t + 1$ locating S_2.

Between the time intervals t and $t + \Delta t$, in a fully implicit discrete format, the transient energy equation for coupled radiation and conduction can be written as

$$C\Delta x\frac{T_i^{m+1}-T_i^m}{\Delta t}=\frac{k_{ie}^{m+1}(T_{i+1}^{m+1}-T_i^{m+1})}{(\delta x)_{ie}}-\frac{k_{iw}^{m+1}(T_i^{m+1}-T_{i-1}^{m+1})}{(\delta x)_{iw}}+\Phi_i^{r,m+1} \tag{1}$$

where Φ^r_i is the radiative source of control-volume i. By the nodal analyzing method, Φ^r_i can be expressed as:

$$\Phi_i^r = q^r_{i,e}(T) - q^r_{i,w}(T) = q^r_{i,e}(T) - q^r_{i-1,e}(T) \tag{2}$$

where $q^r_{i,e}$ is the radiative flux passing through the right interface of control-volume i, and for the gray medium it is written as

$$q^r_{i,e}=\sigma\left\{(n^2_{S_u}[S_uS_v]T_u^4-n^2_{S_v}[S_vS_u]T_v^4)+\sum_{j=1}^{i}(n^2_{S_u}[S_uV_j]T_u^4-n^2[V_jS_u]T_j^4)+\sum_{j=i+1}^{M_t}(n^2[V_jS_v]T_j^4-n^2_{S_v}[S_vV_j]T_v^4)+n^2\sum_{j=i+1}^{M_t}\sum_{l=1}^{i}([V_jV_l]T_j^4-[V_lV_j]T_l^4)\right\} \tag{3}$$

where such as $[S_uS_v]$, $[S_uV_i]$, $[V_iV_j]$, $[S_vV_i]$ and so on are RTCs, deduced by the hybrid ray-tracing method presented in Section 3 of this paper. For the semitransparent boundaries, "S_u" denotes "$S_{+\infty}$" and "S_v" denotes "$S_{-\infty}$", and for the opaque boundaries, "S_u" denotes "S_2" and "S_v" denotes "S_1".

For the semitransparent boundaries, the equation for boundary condition at surface S_1 is written as

$$2k_1(T_1 - T_{S_1})/\Delta x = h_1(T_{S_1} - T_{g_1}) \tag{4}$$

And for the opaque boundaries, it is written as

$$q^r_{S_1} + 2k_1(T_1 - T_{S_1})/\Delta x = \sigma(\varepsilon_1 T^4_{S_1} - T^4_{-\infty}) + h_1(T_{S_1} - T_{g_1}) \tag{5}$$

where $q^r_{S_1}$ is radiative heat flux at S_1 and written as

$$q^r_{S_1}=\sigma n^2\left\{\left([S_2S_1]T^4_{S_2}-[S_1S_2]T^4_{S_1}\right)+\sum_{j=1}^{M_t}\left([V_jS_1]T_j^4-[S_1V_j]T^4_{S_1}\right)\right\} \tag{6}$$

From above equations, major difficulty in coupled radiative–conductive heat transfer problem is the solution to the local radiative source Φ_i^r, and the key to solving Φ_i^r, according to Eq. (3), is in deducing the RTCs.

3. A hybrid ray-tracing method for the deduction of RTC

RTC of element i (surface element or volume element) with respect to element j is defined as quotient of the radiative energy absorbed by element j to the radiative energy emitted by element i. When rays hit a specular surface at an angle, the angle of reflection is equal to the angle of incidence; therefore, the radiative transfer in a medium having specular surfaces can be directionally traced [20]. When rays strike a diffuse surface at an angle, the reflected rays are distributed uniformly over all hemispherical space and the angle of reflection is not always equal to the angle of incidence; therefore, the radiative transfer in a medium having diffuse surfaces cannot be directionally traced. In this case all the incident rays from hemispherical space can be traced to study the radiative transfer [21]. In Ref. [20], RTCs for the medium having specular surfaces were deduced by the directional ray-tracing method, and in Ref. [21], RTCs for the medium having diffuse surfaces were deduced by the hemispherical ray-tracing method. In present work, based on the different reflection characteristics of specular surfaces and diffuse surfaces, a hybrid ray-tracing method is proposed to deduce the RTCs for the medium having S–D surfaces. An absorbing RTC for opaque boundaries, for example (S_1S_2), is taken as an example to illustrate the deduction of RTCs using the hybrid ray-tracing method. According to the radiative transfer mechanism for anisotropic scattering medium [20] and using the hybrid ray-tracing method, the scattering RTC $[S_1S_2]$ can be also deduced, and the deduction is not given in this paper.

Let us first give two expressions for the deduction of RTC (S_1S_2) for convenience:

$$f(x,\theta) = \exp(-\kappa x/\cos\theta) \tag{7}$$

$$F(x) = 2\int_0^{\pi/2} f(x,\theta)\sin\theta\cos\theta \mathrm{d}\theta \tag{8}$$

The energy emitted by the specular surface S_1 transfers through the medium between two surfaces S_1 and S_2, and is finally absorbed by the medium and the surfaces. Now we analyze the transfer process for the energy quotient absorbed by S_2. The transfer process includes two sub-processes: (1) the sub-process of the energy emitted by specular surface getting to diffuse surface, and (2) the sub-process of the energy emitted by diffuse surface getting back to diffuse surface after being reflected by the specular surface. These two sub-processes constitute a complete process of radiant energy transfer from S_1 to S_2, as seen in Fig. 1.

Let us first analyze the first transfer sub-process. The quotient of the radiant energy emitted by the specular surface S_1 at an angle of θ getting to the diffuse surface S_2 for the first time is

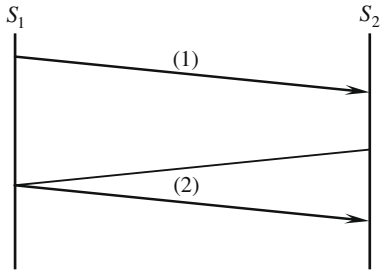

Fig. 1. Sketch for two sub-processes of the radiant energy emitted by S_1 transferring to S_2.

$$(S_1S_2)_1 = f(L,\theta)$$

Then we examine the second transfer sub-process. The radiant energy emitted by the diffuse surface S_2 at an angle of θ first gets to the specular surface S_1, and after being reflected by S_1, it finally gets back to S_2. The quotient of radiant energy with a emission angle of θ carried in this sub-process is $f(L,\theta)\rho_1 f(L,\theta)$. So the quotient of radiant energy emitted by the diffuse surface S_2 that is distributed uniformly over all hemispherical space getting to the specular surface S_1 and finally getting back to S_2 after being reflected is

$$2\int_0^{\pi/2} f(L,\theta)\rho_1 f(L,\theta)\sin\theta\cos\theta \mathrm{d}\theta = \rho_1 F(2L)$$

According to the above analysis, we can obtain the quotient of the radiant energy emitted by S_1 at an angle of θ reaching S_2 for the second time $(S_1S_2)_2 = f(L,\theta)\rho_2\rho_1 F(2L)$. By the similar analysis, we can obtain the energy quotient getting to S_2 for the third time

$$(S_1S_2)_3 = f(L,\theta)\rho_2\rho_1 F(2L)\rho_2\rho_1 F(2L)$$

We can also obtain the expressions of $(S_1S_2)_4$, $(S_1S_2)_5$ and so on.

It is obvious that the series of $(S_1S_2)_1$, $(S_1S_2)_2$, $(S_1S_2)_3$ and so on is a geometric progression with a common ratio of $\beta = \rho_1\rho_2 F(2L)$ $(\beta < 1)$. As a result, we can have total quotient of radiant energy emitted by S_1 at an angle of θ getting to S_2:

$$\sum_{n=1}^{\infty}(S_1S_2)_n = \frac{f(L,\theta)}{1-\beta}$$

Finally, considering emission of two opaque surfaces, we can get the expression of (S_1S_2) as following

$$(S_1S_2) = 2\varepsilon_1\varepsilon_2\int_0^{\pi/2}\sum_{n=1}^{\infty}(S_1S_2)_n\sin\theta\cos\theta \mathrm{d}\theta = \frac{\varepsilon_1\varepsilon_2 F(L)}{1-\beta} \tag{9}$$

By the similar deduction, we can also obtain $(S_{-\infty}S_{+\infty})$ for semitransparent boundaries. If the specular surface S_1 is semitransparent, the polarized effects of radiation must be considered, and the reflectivity of the specular surface S_1 for polarized parallel and perpendicular incident radiation is determined in Ref. [22]. If the diffuse surface S_2 is semitransparent, the determination of the reflectivity of the diffuse surface S_2 can be seen in Ref. [23].

4. Validation of radiative transfer model and numerical method

4.1. Validation of RTCs

The correctness of RTCs describing the information of radiative transfer could be used to validate the radiative transfer model developed by the hybrid ray-tracing method. From the reversibility of radiative transfer and the conservation of radiant energy, RTCs must satisfy the relations of reciprocity and integrality as follows.

Reciprocity relation for volume element vs. volume element can be written as:

$$[V_iV_j] = [V_jV_i] \tag{10a}$$

If two surfaces S_1 and S_2 are opaque, the reciprocity relation for surface element vs. volume element is

$$[S_uV_i] = [V_iS_u] \tag{10b}$$

and that for surface element vs. surface element is

$$[S_1S_2] = [S_2S_1] \tag{10c}$$

If the two surfaces are semitransparent, the reciprocity relation for surface element vs. volume element can be written as

$$n_{S_{-\infty}}^2[S_{-\infty}V_i] = n^2[V_iS_{-\infty}] \tag{10d}$$

$$(1-\rho_{2,in})[S_{+\infty}V_i] = (1-\rho_{2,out})[V_iS_{+\infty}] \tag{10e}$$

and that for surface element vs. surface element is

$$(1-\rho_{2,out})[S_{-\infty}S_{+\infty}] = (1-\rho_{2,in})[S_{+\infty}S_{-\infty}] \tag{10f}$$

where $\rho_{2,in}$ is the reflectivity of the diffuse surface S_2 facing the medium, and $\rho_{2,out}$ is the reflectivity of the diffuse surface S_2 facing the surrounding. The determination of them can be seen in Ref. [23].

Integrality relations for RTCs can be written as:

$$[V_iS_u] + [V_iS_v] + \sum_{j=1}^{M_t}[V_iV_j] = 4\kappa\eta\Delta x \tag{11a}$$

$$[S_uS_u] + [S_uS_v] + \sum_{j=1}^{M_t}[S_uV_j] = \varepsilon_u \tag{11b}$$

By calculating, Eqs. (10) and (11) are well satisfied with RTCs, which shows that the radiative transfer model for the medium having S–D surfaces developed in this paper is rational and correct.

4.2. Linearization of radiative source term

The radiative source term Φ_i^r is a nonlinear function of T_i, so it must be linearized as follows:

$$\Phi_i^{r,m,n+1} = Sc_i^{m,n+1} + Sp_i^{m,n+1}T_i^{m,n+1} \tag{12}$$

with $Sc_i^{m,n+1} = \Phi_i^{r,m,n} - (d\Phi_i^{r,int}/dT_i)^{m,n}T_i^{m,n}$, and $Sp_i^{m,n+1} = (d\Phi_i^r/dT_i)^{m,n}$, where the superscript " m " denotes the " mth " time step, and " n " denotes the " nth " iteration in the " mth " time step. After linearization of the nonlinear term in Eq. (1), linear equations may be obtained and solved by TDMA (Tri-Diagonal Matrix Algorithm) to get temperatures at all nodes.

5. Transient radiative heat transfer

A plane-parallel slab of semitransparent participating medium having two opaque or semitransparent surfaces with $L = 0.02$ m and $C = 0.1\times10^6$ J m^{-3} K^{-1} is considered. Using the first three terms of Legendre polynomial series expansion approximates the characteristics of the anisotropic scattering within a semitransparent material and the general mathematical expression for various scattering phase functions is given as below:

$$\Phi(\theta,\theta_s) = 1 + a_1\cos\theta\cos\theta_s + \frac{1}{4}a_2(3\cos^2\theta-1)(3\cos^2\theta_s-1) \tag{13}$$

where θ is incident angle and θ_s is scattering angle. The case $a_1 = 0$ and $a_2 = 0$ corresponds to isotropic scattering phase function Φ_0, $a_1 = 1$ and $a_2 = 0$ to fully forward scattering phase function Φ_1, $a_1 = -1$ and $a_2 = 0$ to fully backward scattering phase function Φ_2, $a_1 = 0$ and $a_2 = \frac{1}{2}$ to Rayleigh scattering phase function Φ_3, and forward mixed scattering phase function Φ_4 is defined as the case of $a_1 = 1.5$ and $a_2 = \frac{1}{2}$. The effects of scattering albedo, opaque surface emissivity and anisotropic scattering on steady-state heat flux and transient temperature distributions are analyzed in this section.

5.1. Effects of scattering albedo

Parameters for this calculation are taken as: $\tau = 2.0$, $n = 2.0$, $T_0 = 500$ K, $T_{+\infty} = T_{g1} = T_{g2} = 500$ K, $T_{-\infty} = T_r = 1200$ K, $N = 0.005$, and $H_1 = 2.0$, $H_2 = 0$. The medium is considered to be Rayleigh scattering of radiation and has two semitransparent surfaces. Transient heat transfer is examined for different scattering albedoes such as $\omega = 0.1$ and $\omega = 0.9$. In this section, the results of "S–S", obtained by the ray-tracing method [20], is for the medium with two specular surfaces, and the results of "S–D", obtained by the hybrid ray-tracing method, is for the medium having one specular surface and the other diffuse surface.

Radiation emitted by black surrounding $S_{-\infty}$ with high temperature can penetrate the semitransparent surface S_1 and transfers within the medium. The left surface of the medium is radiatively heated by black surrounding $S_{-\infty}$ and simultaneously cooled by convection, which results in temperature peaks appearing in the areas close to S_1, as shown in Fig. 2. In the medium having a small scattering albedo of 0.1, temperature profiles for the areas close to the radiatively heating surface S_1 is very steep, plotted in Fig. 2a. If the scattering albedo is so big, for example $\omega = 0.9$, the corresponding temperature curves become somewhat gentle, seen in Fig. 2b. From Fig. 2, we can also observed that the transient temperature peak at a certain time is smaller and steady temperature peak is bigger for the medium with big scattering albedo compared to the medium having small scattering albedo.

Table 1 shows the effects of scattering albedo on steady total heat flux. It is noted that from Table 1 with the increase of scattering albedo, total heat flux in steady-state increases, and the relative heat flux difference decreases between media with S–D surfaces and S–S surfaces.

From Fig. 2 and Table 1 it can be further observed that temperature curves for the medium with S–D surfaces are higher than those for the medium having S–S surfaces at any time, and in steady-state, total heat flux through the medium with S–D surfaces is smaller than that with S–S surfaces. It is shown that in the medium

Table 1
Dimensionless heat flux in steady-state for various values of scattering albedo, $q^t/\sigma T_r^4$.

$\omega = 0.1$		$\omega = 0.9$	
S–D	S–S	S–D	S–S
0.29710	0.33420	0.34905	0.38645

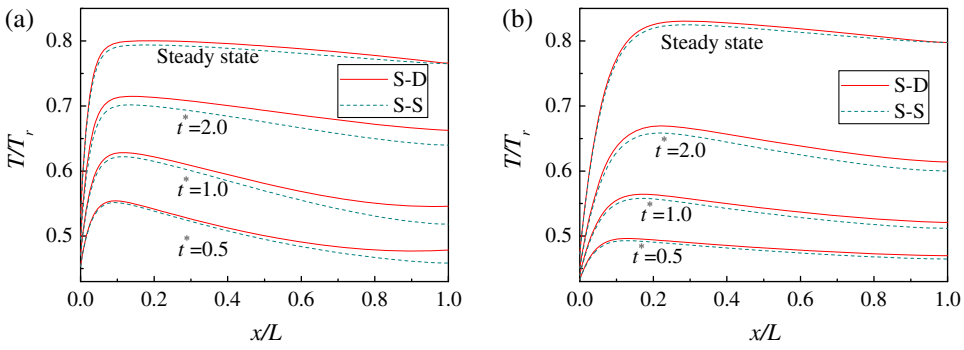

Fig. 2. Effects of scattering albedo on transient temperature distributions in a Rayleigh scattering medium: (a) $\omega = 0.1$ and (b) $\omega = 0.9$.

having two semitransparent surfaces, the diffuse reflection can weaken radiative heat transfer compared to the specular reflection.

5.2. Effects of diffuse surface emissivity

In this section, calculation parameters are taken as: $\tau = 2.0$, $n = 2.0$, $\omega = 0.5$, $T_0 = 750$ K, $T_{+\infty} = T_{g2} = T_r = 1500$ K, $T_{-\infty} = T_{g1} = 750$ K, $N = 0.05$ and $H_1 = \infty$, $H_2 = 2.0$. Rayleigh scattering is considered and two surfaces are supposed to be opaque. The effect of diffuse surface emissivity on the coupled radiative and conductive heat transfer is investigated as following.

The specular surface S_1 is cooled by convection and radiates heat to the left black surrounding $S_{-\infty}$, and the diffuse surface S_2 is irradiated by the right black surrounding $S_{+\infty}$ with high temperature and heated by convection. S_2 partly absorbs the external radiation emitted by $S_{+\infty}$ and heats the medium by coupled radiation and conduction. From Fig. 3 we can see that the temperature distributions in the medium having a bigger ε_2 are always higher than those having a smaller ε_2, resulting from more external radiation being absorbed by the surface with a bigger ε_2. Steady radiative heat flux through the medium with a bigger ε_2 is also observed to be larger than that with a smaller ε_2.

5.3. Effects of anisotropic scattering

Common parameters of thermal properties and radiative properties are taken as: $\omega = 0.9$, $N = 0.005$, and $H_1 = 1.0$, $H_2 = 1.0$, and temperatures as input data are taken as: $T_0 = 500$ K, $T_{-\infty} = T_{g1} =$!500 K, $T_{+\infty} = T_{g2} = T_r = 1500$ K. The medium under consideration is supposed to have two semitransparent S–D surfaces. The effects of anisotropic scattering characteristics are examined on transient coupled heat transfer dominated by radiation when the right surface S_2 is heated by convection and irradiation.

Fig. 4 gives the results for $\tau = 2.0$ and $n = 2.0$, Figs. 5 and 6 plot the results for $\tau = 20$, and Table 2 tabulates the results for $n = 2.0$. For the bigger refractive indices such as $n = 2.0$ and $n = 5.0$, as seen in Figs. 4a and 5b and c, in different areas of the media having different scattering phase functions, the temperatures have different distribution characteristics. In areas close to the right hot surface S_2, the temperature distribution for scattering phase function Φ_2 is highest, followed by Φ_3, and the lowest temperature distribution is for scattering phase function Φ_4. In the left areas away from S_2, the opposite trend is observed, and the temperature distribution difference is larger between media having different scattering phase functions compared to the right areas close to S_2. Comparing Fig. 4a with Fig. 5b, we can see that the temperature distribution characteristics are more significant for bigger optical thickness. For the same optical thickness, refractive index affects temperature distributions in media having different scattering phase functions so much. For a small refractive index, for example, $n = 1.1$, from Fig. 5a it is seen that in entire region of the medium the temperature distributions for Φ_4 are highest, followed by Φ_1, and for Φ_2 it is lowest. As the refractive index increases, the curves of temperature distribution in media having different phase functions intersect each other in the areas close to the hot surface S_2. From Fig. 5b and c it is observed that in the region at the right of the point of intersection, temperature curves for Φ_4 are lowest and those for Φ_2 are highest; in the region at the left of the point of intersection, the temperature distribution characteristics are opposite to the right region. From Fig. 5b and c, we also find that the smaller the refractive index is, the smaller the right region is. When the refractive index is small enough, the right region where the temperature curves for Φ_4 are lowest and those for Φ_2 are highest disappears, as seen in Fig. 5a. Comparing Fig. 4 with Fig. 5 we find that the increase of optical thickness can enhance the effects of anisotropic scattering; for the same optical thickness,

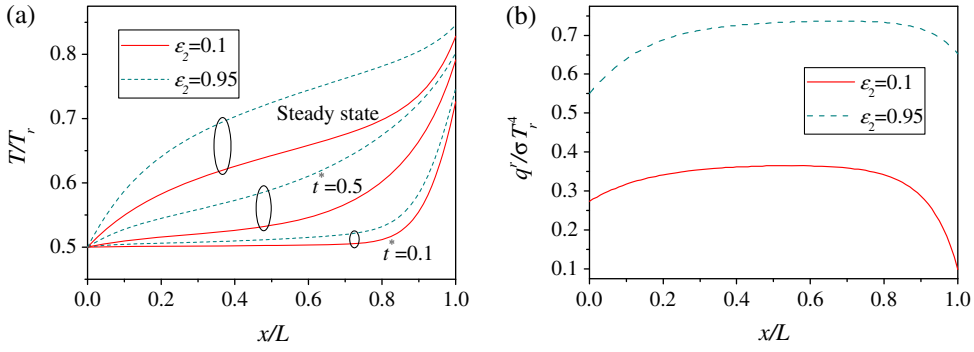

Fig. 3. Effects of emissivity on coupled heat transfer in a Rayleigh scattering medium: (a) transient temperature distributions, and (b) dimensionless radiative flux in steady-state.

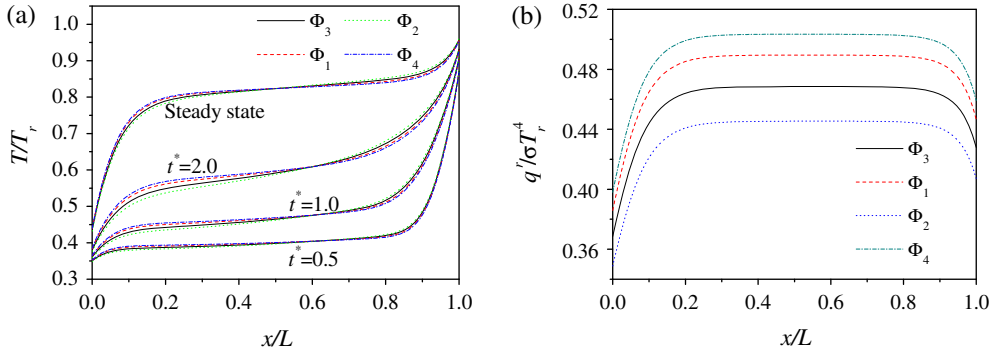

Fig. 4. Effects of anisotropic scattering on coupled heat transfer in a medium: (a) transient temperature distributions, and (b) dimensionless radiative flux in steady-state.

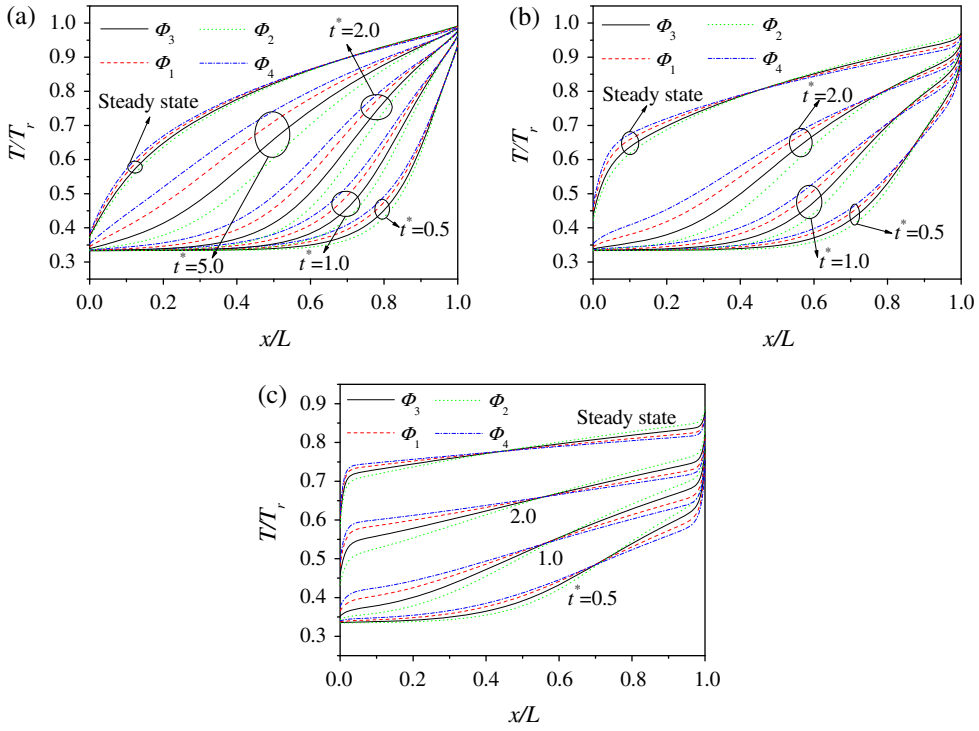

Fig. 5. Effects of anisotropic scattering on transient temperature distributions in a medium for different refractive indexes: (a) $n = 1.1$, (b) $n = 2.0$, and (c) $n = 5.0$.

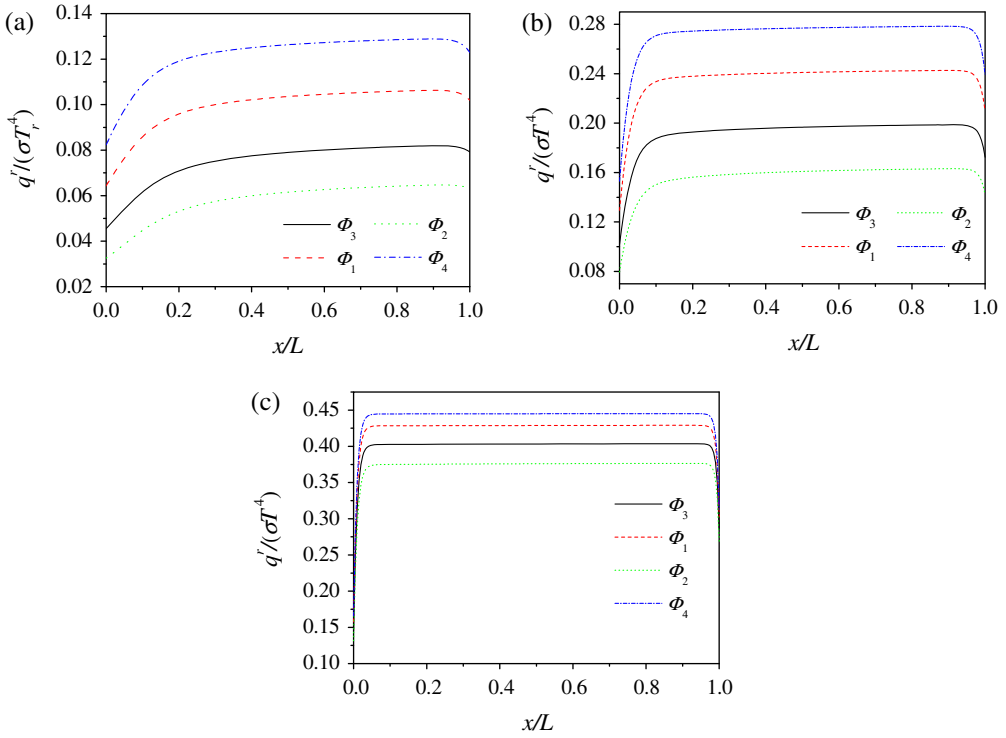

Fig. 6. Effects of anisotropic scattering on radiative flux distributions in steady-state in a medium for different refractive indexes: (a) $n = 1.1$, (b) $n = 2.0$, and (c) $n = 5.0$.

Table 2
Effects of anisotropic scattering on dimensionless heat flux $q^r/\sigma T_r^4$ in steady-state for different optical thickness.

$\tau = \kappa L = 2.0$				$\tau = \kappa L = 20.0$			
Φ_1	Φ_2	Φ_3	Φ_4	Φ_1	Φ_2	Φ_3	Φ_4
0.49062	0.44729	0.46999	0.50432	0.24693	0.16796	0.20327	0.28239

the smaller the refractive index is, the more the anisotropic scattering affects transient temperature distributions in the medium. Next, we discuss the effects of anisotropic scattering on the heat flux. From Figs. 4b and 6 it is found that in the medium having different phase functions, the curves of steady radiative flux for Φ_4 is highest, followed by Φ_1, and that for Φ_2 is lowest. The same changing law with different phase functions can be observed for steady total heat flux from Table 2. Relative to temperature distributions, anisotropic scattering has a more influence on the distributions of heat flux. In addition, when the refractive index is large, as shown in Fig. 6c, the steady-state radiative heat flux changes rapidly in the regions near the surfaces, and the curves of radiative heat flux through central regions can be approximated as straight lines.

6. Conclusions

According to the different reflecting characteristics of specular surface and diffuse surface, a hybrid ray-tracing method is developed for the solution to radiative transfer inside a medium having one specular surface and the other diffuse surface. By this method the RTCs for specular–diffuse surfaces is deduced and the corresponding radiative heat source in energy equation for coupled radiation and conduction is obtained. The effects of scattering albedo, diffuse surface emissivity and anisotropic scattering on transient temperature distributions and steady-state heat flux are investigated. From the results obtained above we may draw some conclusions as follows.

(1) In the medium having two semitransparent surfaces, the diffuse reflection can weaken radiative heat transfer compared to the specular reflection, which results in temperature curves for the medium with S–D surfaces higher than those for the medium having S–S surfaces at any time.
(2) In the medium with semitransparent surfaces, a bigger scattering albedo can cause smaller temperature peaks in transients, but at steady-state, it can cause larger temperature peaks.
(3) Increase of the optical thickness can enhance the effects of anisotropic scattering; and for the medium having the same optical thickness, the smaller the refractive index is, the more the anisotropic scattering affects transient temperature distributions. When the refractive index is very small, in entire regions of the medium, temperature curves for forwardly scattering phase functions are higher than those for backwardly scattering phase functions. Distribution curves of radiative heat flux for forwardly scattering phase functions are higher than those for backwardly scattering phase functions, regardless of the values of refractive index.

Acknowledgments

The support of this work by the Major Program of International Cooperation of National Natural Science Foundation of China (No. 50620120442) and the National Natural Science Foundation of China (No. 50806018) are gratefully acknowledged.

References

[1] J.M. Goyheneche, J.F. Sacadura, The zone method: a new explicit matrix relation to calculate the total exchange areas in anisotropically scattering medium bounded by anisotropically reflecting walls, J. Heat Transfer – Trans. ASME 124 (2002) 696–703.
[2] F. Dupoirieux, L. Tesse, S. Avila, J. Taine, An optimized reciprocity Monte Carlo method for the calculation of radiative transfer in media of various optical thicknesses, Int. J. Heat Mass Transfer 49 (2006) 1310–1319.
[3] M.A. Atalay, P–N solutions of radiative heat transfer in a slab with reflective boundaries, J. Quant. Spectrosc. Radiat. Transfer 101 (1) (2006) 100–108.
[4] B. Mondal, S.C. Mishra, Application of the lattice Boltzmann method and the discrete ordinates method for solving transient conduction and radiation heat transfer problems, Numer. Heat Transfer A – Appl. 52 (2007) 757–775.
[5] S.C. Mishra, A. Lankadasu, Transient conduction–radiation heat transfer in participating media using the lattice Boltzmann method and the discrete transfer method, Numer. Heat Transfer A – Appl. 47 (2005) 935–954.
[6] M.Y. Kim, Assessment of the axisymmetric radiative heat transfer in a cylindrical enclosure with the finite volume method, Int. J. Heat Mass Transfer 51 (2008) 5144–5153.
[7] L.H. Liu, L.J. Liu, Discontinuous finite element method for radiative heat transfer in semitransparent graded index medium, J. Quant. Spectrosc. Radiat. Transfer 105 (2007) 377–387.
[8] H. Sadat, On the use of a meshless method for solving radiative transfer with the discrete ordinates formulations, J. Quant. Spectrosc. Radiat. Transfer 101 (2006) 263–268.
[9] M. Ben Salah, F. Askri, K. Slimi, S. Ben Nasrallah, Numerical resolution of the radiative transfer equation in a cylindrical enclosure with the finite-volume method, Int. J. Heat Mass Transfer 47 (10–11) (2004) 2501–2509.
[10] D. Byun, C. Lee, S.W. Baek, Radiative heat transfer in discretely heated irregular geometry with an absorbing, emitting, and anisotropically scattering medium using combined Monte-Carlo and finite volume method, Int. J. Heat Mass Transfer 47 (19–20) (2004) 4195–4203.
[11] D.N. Trivic, T.J. O'Brien, C.H. Amon, Modeling the radiation of anisotropically scattering media by coupling mie theory with finite volume method, Int. J. Heat Mass Transfer 47 (26) (2004) 5765–5780.
[12] D. Sarma, S.C. Mishra, P. Mahanta, Analysis of collimated radiation in participating media using the discrete transfer method, J. Quant. Spectrosc. Radiat. Transfer 96 (1) (2005) 123–135.
[13] H.C. Zhou, Q. Cheng, Z.F. Huang, C. He, The influence of anisotropic scattering on the radiative intensity in a gray, plane-parallel medium calculated by the DRESOR method, J. Quant. Spectrosc. Radiat. Transfer 104 (1) (2007) 99–115.
[14] F. Asllanaj, X. Brige, G. Jeandel, Transient combined radiation and conduction in a one-dimensional non-gray participating medium with anisotropic optical properties subjected to radiative flux at the boundaries, J. Quant. Spectrosc. Radiat. Transfer 107 (1) (2007) 17–29.
[15] B. Mondal, S.C. Mishra, Lattice Boltzmann method applied to the solution of the energy equations of the transient conduction and radiation problems on non-uniform lattices, Int. J. Heat Mass Transfer 51 (1–2) (2008) 68–82.
[16] H.P. Tan, H.C. Zhang, B. Zhen, Estimation of ray effect and false scattering in approximate solution method for thermal radiative transfer equation, Numer. Heat Transfer A 46 (8) (2004) 807–829.
[17] P. Sadooghi, Transient coupled radiative and conductive heat transfer in a semitransparent layer of ceramic, J. Quant. Spectrosc. Radiat. Transfer 92 (4) (2005) 403–416.
[18] B. Safavisohi, E. Sharbati, C. Aghanajafi, S.R.K. Firoozabadi, Effects of boundary conditions on thermal response of a cellulose acetate layer using Hottel's zonal method, J. Fusion Energy 25 (3–4) (2006) 145–153.
[19] H.P. Tan, J.F. Luo, X.L. Xia, Q.Z. Yu, Transient coupled heat transfer in multilayer composite with one specular boundary coated, Int. J. Heat Mass Transfer 46 (4) (2003) 731–747.
[20] H.P. Tan, H.L. Yi, P.Y. Wang, L.M. Ruan, T.W. Tong, Ray tracing method for transient coupled heat transfer in an anisotropic scattering layer, Int. J. Heat Mass Transfer 47 (19–20) (2004) 4045–4059.
[21] H.L. Yi, H.P. Tan, Y.P. Lu, Effect of reflecting modes on combined heat transfer within an anisotropic scattering slab, J. Quant. Spectrosc. Radiat. Transfer 95 (1) (2005) 1–20.
[22] R. Siegel, J.R. Howell, Thermal Radiation Heat Transfer, fourth ed., Taylor & Francis, New York, London, 2002. p. 85.
[23] R. Siegel, C.M. Spuckler, Refractive index effects on radiation in an absorbing, emitting, and scattering laminated layer, J. Heat Transfer – Trans. ASME 115 (1) (1993) 194–200.